Journal of Hazardous Materials 186 (2011) 1254–1262

Contents lists available at ScienceDirect

Journal of Hazardous Materials

journal homepage: www.elsevier.com/locate/jhazmat

A new approach to simulate characterization of particulate matter employing support vector machines

K. Mogireddy[a], V. Devabhaktuni[a,*], A. Kumar[b], P. Aggarwal[a], P. Bhattacharya[c]

[a] EECS Department, University of Toledo, MS 308, 2801W. Bancroft Street, Toledo, OH 43606, USA
[b] Department of Civil Engineering, University of Toledo, MS 307, 2801W. Bancroft Street, Toledo, OH 43606, USA
[c] School of Computing Sciences & Informatics, Univ. of Cincinnati, 814B Rhodes Hall, Cincinnati, OH 45221, USA

ARTICLE INFO

Article history:
Received 8 November 2010
Received in revised form
22 November 2010
Accepted 30 November 2010
Available online 7 December 2010

Keywords:
Particulate matter (PM)
Support vector machines (SVMs)
Scanning electron microscope (SEM)
Image processing

ABSTRACT

This paper, for the first time, applies the support vector machines (SVMs) paradigm to identify the optimal segmentation algorithm for physical characterization of particulate matter. Size of the particles is an essential component of physical characterization as larger particles get filtered through nose and throat while smaller particles have detrimental effect on human health. Typical particulate characterization processes involve image reading, preprocessing, segmentation, feature extraction, and representation. Of these various steps, knowledge based selection of optimal image segmentation algorithm (from existing segmentation algorithms) is the key for accurately analyzing the captured images of fine particulate matter. Motivated by the emerging machine-learning concepts, we present a new framework for automating the selection of optimal image segmentation algorithm employing SVMs trained and validated with image feature data. Results show that the SVM method accurately predicts the best segmentation algorithm. As well, an image processing algorithm based on Sobel edge detection is developed and illustrated.

1. Introduction

Particulate matter (PM) is a complex mixture of minute solid particles and liquid droplets found in air [1]. It consists of a number of components such as acids, organic chemicals, metals, and soil or dust particles. Typically, these particles can arise from natural sources (*e.g.* volcanoes, dust storms, forest fires, etc.) as well as human activities (*e.g.* burning of fossil fuels in vehicles, power plants, etc.).

Behavior of such particles in air and in human body is dependent on their physical as well as chemical characteristics. Physical properties, *e.g.* size/shape, determine the time the particle remains airborne and its penetration/deposition in human respiratory tract [2]. Morphological parameters establish the atmospheric behavior of particulate matter and their effect on human health [6]. For example, particles having aerodynamic diameter greater than 10 μm typically get filtered in the nose and throat, and do not cause problems, but PM_{10} (with aerodynamic diameter less than 10 μm) can easily enter the lungs and cause severe health problems. Fine $PM_{2.5}$ (with diameters in the range of 0.1–2.5 μm) can penetrate deep into the lungs [3–5] and may damage alveolar tissues. Extremely small particles with diameters less than 100 nm may affect other vital organs such as brain. Shape is one of the major physical properties of PM determining the effect on human health [7]. Geometrically speaking, angular shapes have more surface area compared to round shapes. This increases the PM binding capacity to other harmful substances. Shandilya and Kumar [8] studied the morphology of particles present in a bio-diesel bus and characterized the particles into 14 shapes. In essence, characterization of particulate matter is an important field from the viewpoint of both environment and human health.

Several approaches have been developed for analyzing the physical and chemical properties of particulate matter. The gravimetric method quantitatively determines the chemical substances present in the particles and is based on the mass of a substance. However, it usually provides the chemical analysis of a single element, or a group of elements, at a time [9]. Atomic absorption spectroscopy is a technique that measures the absorption of radiation as function of frequency or wavelength [10]. While this method can identify most of the metals in the periodic table, it is not able to determine size or shape of the particles. High performance liquid chromatography (HPLC) extracts the chemical compound from mixture of compounds based on polarity [11]. It is an automated process that takes only a few minutes to produce results. However, it requires trained technicians to operate expensive machinery. Gas chromatogra-

* Corresponding author. Tel.: +1 419 530 8172; fax: +1 419 530 8146.
E-mail addresses: Kranthi.Mogireddy@rockets.utoledo.edu (K. Mogireddy), Vijay.Devabhaktuni@utoledo.edu (V. Devabhaktuni), Ashok.Kumar@utoledo.edu (A. Kumar), Priyanka.Aggarwal@utoledo.edu (P. Aggarwal), bhattapr@ucmail.uc.edu (P. Bhattacharya).

0304-3894/$ – see front matter © 2010 Elsevier B.V. All rights reserved.
doi:10.1016/j.jhazmat.2010.11.129

phy/mass spectrometry (GC/MS) is a method that combines the features of GC and MS for identifying various chemical substances present in a test sample [12,13]. However, this technique can only be used for chemical characterization. Another method involves observing the collected particles through optical microscope so as to measure their size [14]. Here, the particles are counted/measured until stable size distribution range is obtained. This is a low-cost system but involves slow counting process [14].

The state-of-the-art has progressed toward employing scanning electron microscope (SEM) with energy dispersive X-ray (EDX) method that uses electrons to provide magnified images, better feature resolution, and a greater depth-of-field in contrast to light microscopes [15–17]. The spatial resolving power of the SEM technique is in the submicron level making it well-suited for PM_{10} analysis. SEM/EDX method can be performed in three different ways—Manual SEM, Computer Controlled SEM (CCSEM) method [18], and SEM integrated with image analyzing software techniques [19]. The first attempt to use image processing for PM began in the mid 80s, while development accelerated in the mid 90s with the emergence of high-computational power and highly sophisticated microscopes. The inclination is to use modern image analysis systems with capabilities of analyzing thousands of particles (less than 1 μm) in a matter of minutes [20].

While these developments continued on the image acquisition and processing front, another area that emerged with applications in wide engineering and scientific disciplines is machine learning. For example, artificial neural networks have been applied to converting human-intensive tasks to automated computer-tasks. One of the disadvantages of neural networks is the requirement for a relatively larger training data. However, collection of environmental samples is often expensive. Motivated by these observations, this paper applies a new machine leaning paradigm, *i.e.* SVMs, for automating the selection of optimal image segmentation algorithm. Unlike neural networks, SVMs require significantly fewer training data.

Section 2 describes the basic image processing steps involved in the characterization of PM from captured images. Section 3 presents the developed extended Sobel edge detection method, while section 4 presents a comparison of commercially available particle image analysis software tools. Section 5 presents an approach to automatic selection of optimal image segmentation algorithm employing SVMs. Finally, Section 6 concludes the paper.

2. Principle of PM characterization by SEM integrated with image analyzing techniques

Analyzing the SEM images (after the images have been acquired) for particle characterization consists of five steps: image reading, preprocessing, segmentation, feature extraction, and representation [21].

2.1. Image reading

Image reading converts the particle image into formatted numerical values, which are then processed by a computer. Images are represented as two-dimensional (2D) array of points called pixels. Each pixel represents the irradiance at the corresponding grid position. The position of the pixel is specified by $M \times N$ matrices, where M and N denotes the position of the pixel in Mth row and Nth column.

2.2. Preprocessing

This step improves the quality of the captured image before further analysis can be performed. The preprocessing step may include noise reduction, contrast enhancement, etc. Noise reduction is the process of removing/reducing imperfections such as unwanted dots, lines, smudges from the images while contrast enhancement increases the contrast between object (particle) and background (filter paper).

2.3. Segmentation

Segmentation is the most vital step in analyzing images for PM characterization. Segmentation refers to the process of partitioning a digital image into multiple segments (sets of pixels) [21]. Typically, segmentation locates objects and boundaries (lines, curves, etc.) in images so as to identify particles in the image. In other words, segmentation is the process of assigning a label to every pixel in an image such that the pixels with the same labels share similar visual characteristics [22].

For particle images, segmentation methods should accurately separate particle pixels from background pixels. Currently, there are many segmentation techniques but most of these do not yield satisfactory results for all types of images, *i.e.,* one segmentation algorithm may not give the best result for all kind of images. Some important segmentation algorithms and their best suited images are depicted in Table 1. One of the main challenges during segmentation is separating the connected particles present in the images as it will readily change the estimate of its physical characteristics such as count, size, shape. Techniques like Watershed [20], Skeltonization by Influence Zone (SKIZ) [20], fuzzy c-mean segmentation (FCM) [23], can be used to separate the connected particles.

2.4. Feature extraction

After separating the particles from the background in an image, particle features have to be extracted. First, the connected component labeling algorithm [24–26] is used to uniquely label each particle present in image and then size, area, and other features of particles are determined. As particles are irregular in shape, we define the size of particle as the longest distance between two edges of the particle. Finding the shape of the particle is a difficult problem and is separately discussed in Section 2.4.1.

2.4.1. Shape of PM

Particle shape analysis is one of the most difficult problems in PM characterization. The shape factor or form factor (ff) is one of the parameters that characterize the shape of an object [27]. It compares the object's area (A) to its perimeter (P) and is defined by:

$$ff = \frac{4\pi A}{P^2}. \quad (1)$$

Smooth and round objects have a form factor close to unity while elongated objects have a smaller form factor ($0 < ff < 1$). The area is evaluated by enumerating the number of pixels inside the object. The perimeter of particle is determined by counting the number of pixels along the particle's border.

2.5. Representation

Data such as the size and shape of particles present in filter paper is processed by conventional statistical methods, and the results can be represented by various types of graphs, histograms, and tables.

To demonstrate the use of image processing algorithm for physical characterization of PM, an image processing algorithm is developed based on the extended Sobel edge detection method. This algorithm is discussed in Section 3.

Table 1
Different segmentation algorithms.

Method	Suitable image	Segmentation effect	Comments
Minimum thresholding	Images with high intensity difference between object and background	Normal	Narrow application area
Iterative thresholding	All type of images	Good	Sensitive to noise
Entropy based thresholding	Images with low contrast and complex background	Normal	Sensitive to noise
Otsu thresholding	Images with bi-modal histogram	Good	Does not work well with images with non-uniform illumination
Genetic algorithm	All types of images	Normal	Performance can be increased by optimizing adaptability function
Genetic algorithm with Otsu	All types of images	Excellent	Speed is slow
Edge based segmentation	Images having sharp edges	Good	Edges identified by edge detection are often disconnected, closed regions required for object segmentation
Fuzzy clustering segmentation	All types of images	Good	Quality of the final solution depends on initial cluster set
Iterative fuzzy segmentation	All types of images	Good	Segmentation speed is slow
Neural network based segmentation	All types of images	Good	Has fast computing capability and less sensitive to noise, but requires extensive training
Watershed segmentation	All types of images	Normal	Leads to over segmentation

3. Extended Sobel edge detection method for particle characterization

To start with, the noise present in the image is reduced by using a median filter. The median filter is a nonlinear digital filtering method that reduces noise while preserving the edges. A median filter replaces each pixel's intensity value in an image with a median value calculated in small window, with size say 3×3 pixels. Then, the edges of the particles present in image are identified by using the Sobel edge detection operator [35]. The Sobel operator calculates the gradient of the image intensity at each pixel, i.e. it calculates the directional change in the intensity for each pixel. After the gradient image has been computed, pixels with large gradient values become edge pixels. Mathematically, the operator uses two 3×3 kernels (these are the matrices shown in (2)) which are convolved with the original image to calculate the approximation of the derivatives, one for horizontal change and the other for vertical change [26]. If, I is assumed as source image, then G_x and G_y are two images that contain the horizontal and vertical derivative approximations, and are computed using (2). At each pixel in the image, the resulting horizontal and vertical gradient approximation can be combined to give the gradient magnitude of the Sobel operated image using (3).

$$G_x = \begin{bmatrix} -1 & 0 & 1 \\ -2 & 0 & 2 \\ 1 & 0 & 1 \end{bmatrix} * I \quad \text{and} \quad G_y = \begin{bmatrix} -1 & -2 & -1 \\ 0 & 0 & 0 \\ 1 & 2 & 1 \end{bmatrix} * I, \tag{2}$$

where * denotes the convolution operation.

$$G = \sqrt{G_x^2 + G_y^2}. \tag{3}$$

The Sobel operation results in lines of high contrast across the boundary regions of particles. However, these lines do not quite describe the outline of the particles in an image as there can be gaps in the particles contour. These linear gaps are removed by using a dilation operator which uses a structuring element (small sets or sub-images used to interact with the image) for expanding the boundaries of foreground pixels in the image [26]. Dilation of image I using a structuring element B ($I \oplus B$) is given by:

$$I \oplus B = \{Z | [(\hat{B})_z \cap I] \subseteq I\}, \tag{4}$$

where $(\hat{B})_z$ is reflection of B about its origin shifted by z.

After dilation, particle holes are filled using the region filling algorithm, based on (5) [26].

$$I_m = (I_{m-1} \oplus B) \cap A^c, \tag{5}$$

Table 2
SEM setting used for capturing images.

Acceleration voltage (keV)	30
Magnification	201
Working distance (mm)	8.8
Detector	BSE

where $m = 1, 2, 3, \ldots, M$, the algorithm terminates at iteration step M if $I_M = I_{M-1}$. $I_0 = p$, p is the point inside the boundary of the particle, A denotes a set containing a subset whose elements are 8-connected boundary points of the particle.

Further, the connected component labeling method is used to count the number of particles in the image by labeling each particle in the image uniquely. Finally, the physical characteristics of the particles are determined as discussed in Section 2.4. The image shown in Fig. 1(a) and other images used in this paper are the images of the filter paper captured using FEI Quanta 3D SEM. The settings of the SEM are shown in Table 2. Particles present on the filter paper appear as bright spots in the images. Particles are collected on the filter papers using GRIMM 1.108 aerosols counter during the application of biosolids on farm fields of Ohio.

Various commercially available image analyzing software for PM characterization are discussed in Section 4.

4. Commercial software for integrating SEM and image analyzing techniques for PM characterization

Various commercial software are available for analyzing the particle images obtained from SEM. The software can identify the particles present in the image and also determine size, shape, and other features of the particle. ImageJ [28] and Scanning Probe Image Processor (SPIP) [29] are the most popular software used for analyzing the SEM images. Software such as PAX-it [30], Clemex Vision PE [31], SmartPI [32], and Image Pro [33] can automate the SEM controls for capturing images and also analyze images automatically.

Two main drawbacks of commercial image software are: inability to identify overlapped particles and non-automatic selection of segmentation algorithms. When overlapped particles appear in particle images, the existing software treats it as a single particle, which leads to incorrect physical characterization of these particles. Various image processing techniques such as watershed segmentation, SKIZ and fuzzy clustering [23] methods are reported to separate these overlapped particles.

Another drawback of image analyzing software is the inability to automatically determine the best segmentation method for a given image. For each image, the segmentation algorithm is manu-

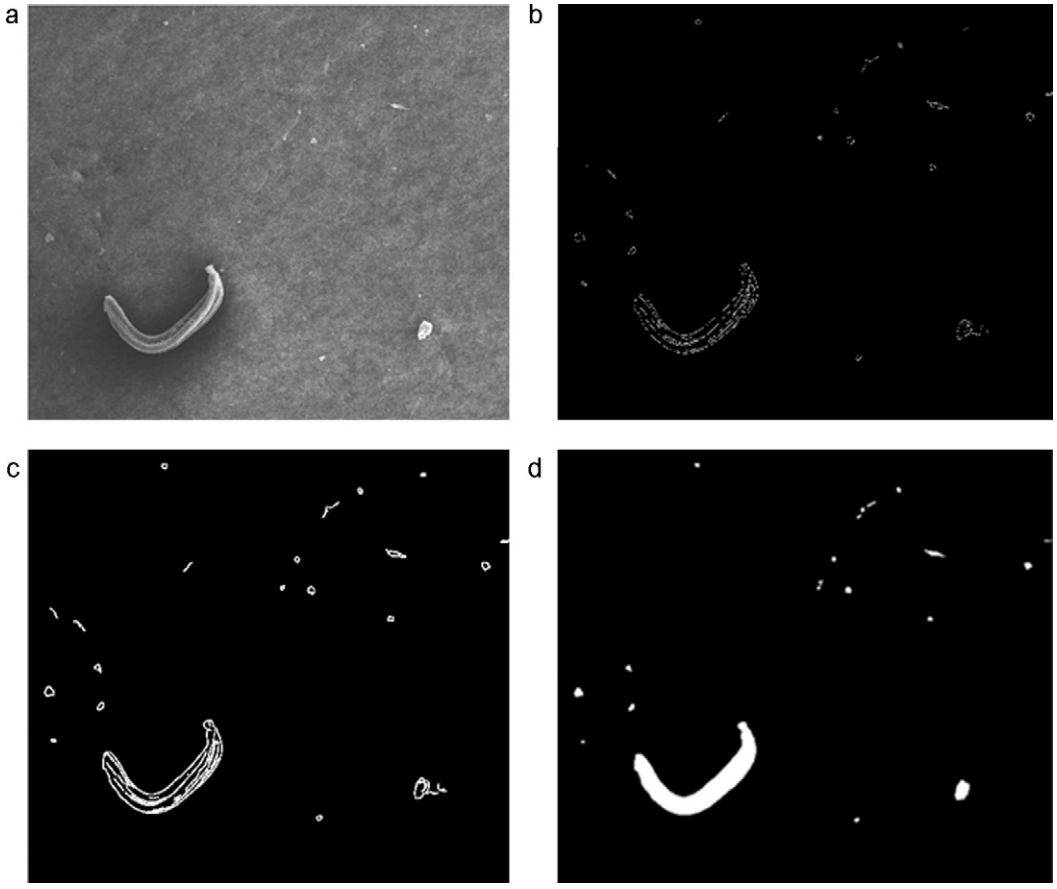

Fig. 1. Example to illustrate the extended Sobel edge detection method: (a) SEM image of a particulate filter paper, (b) image after applying the Sobel operator, (c) image after applying dilation operator, (d) final output image showing filled particles.

ally selected from a stack of available algorithms based on the user's experience and knowledge. As previously discussed, each image segmentation algorithm gives satisfactory results for a particular type of image. For PM characterization using SEM integrated with image processing method, automatic selection of suitable segmentation algorithm is required to achieve efficiency and robustness. In this paper, we propose the selection of best image segmentation algorithm for particle images based on SVMs. The proposed method is based on the fact that there exists a strong correlation between image features and the performance of segmentation algorithm [34]. Support vector machines have the capability of interpreting images like humans and use image features for automatically predicting best image segmentation algorithm [35] as discussed in Section 5.

5. Selection of optimal image segmentation algorithm by support vector machines

Support vector machines are a set of related supervised learning methods developed by Vapnik and his colleagues [36]. The SVM constructs a hyperplane or set of hyperplanes in a high or infinite dimensional space, which can be used for classification, regression and other tasks. Basic linear separating hyperplane for a two class problem is shown in Fig. 2(a). Given a set of training examples

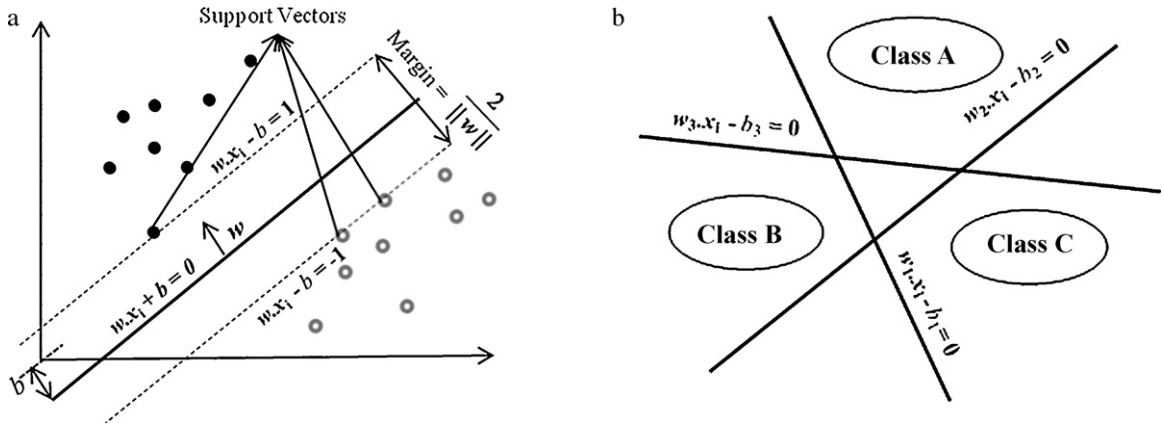

Fig. 2. (a) Basic linear separation hyperplane for two class problems and (b) multiclass classification by SVM.

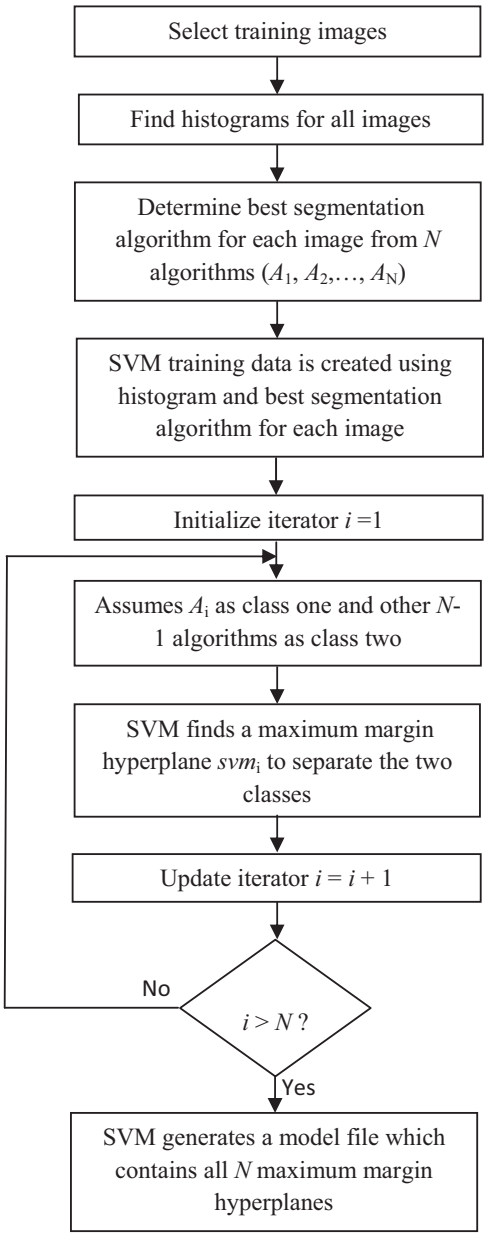

Fig. 3. SVM training algorithm.

belonging to two different categories, an SVM training algorithm builds a model that predicts which class a new image falls into.

A SVM is used as learning based technique for predicting the suitable segmentation algorithm for an image based on its features like a gray level histogram. Selection of the optimal image segmentation algorithm using an SVM has two stages, training and validating. In the training stage, a database is created using random images along with the optimal segmentation algorithm for those images. Then the SVM is fed with this shaped database. The SVM classifies the training images into different classes by constructing hyperplanes such that images having similar features belong to a class, thereby learning the relationship between image features and segmentation algorithms. It is assumed that the application of a segmentation algorithm to all images belonging to a class will show comparable performance. In the validation stage, the SVM evaluates a particular class based on its previous training and thus predicts the suitable segmentation algorithm.

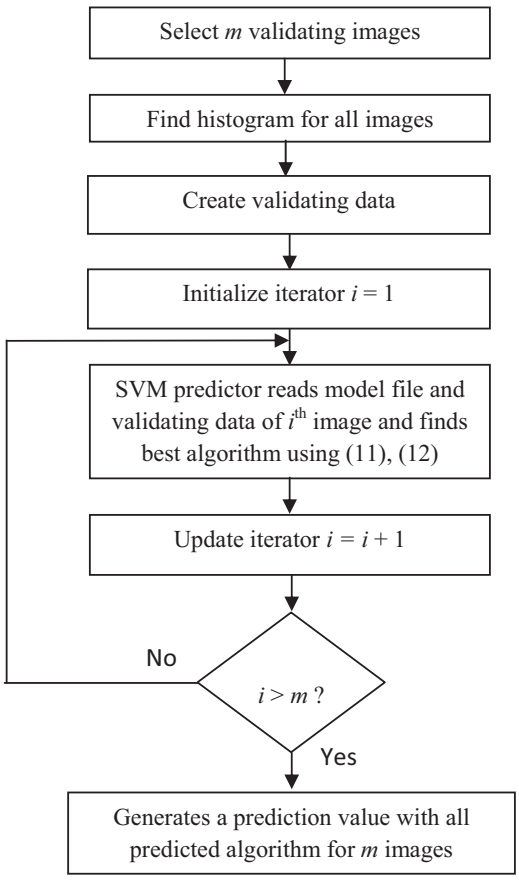

Fig. 4. SVM validating algorithm.

Support vector machines are of two types, namely, linear SVM and nonlinear SVM. Basically, SVMs are designed for binary classification problems *i.e.* two-class problems. However it can be extended to a multiclass problem by simplifying it into multiple binary classifications. An example illustrating the multiclass problem is shown in Fig. 2(b). In this paper, the multiclass SVM is used for automating the selection of a suitable image segmentation algorithm for images. Steps followed in training and validating stage are discussed below.

5.1. Training SVM

First in the training stage a set of k images are selected and histogram is determined for all images. Each training image is segmented by all N different segmentation algorithms ($A_1, A_2, \ldots, A_N$), with the goal of selecting the best image segmentation algorithm for the image. The steps involve in SVM training is depicted in Fig. 3.

Each algorithm is identified with a positive integer value ranging from 1 to N (number of segmentation algorithm), *i.e.* $A_1 = 1$, $A_2 = 2, \ldots, A_N = N$. Next, the training data for the SVM is created using an image histogram and its associated best segmentation algorithm. This training database is of the form:

$$D = \{(A_1, x_1), (A_2, x_2), \ldots, (A_N, x_k)\}^T, \quad (6)$$

where x_k is the histogram of kth image represented in the form of p-dimensional real vector ('p' is the number of bins into which the image pixel are divided while finding the histogram of an image) and $A_N \in \{1, 2, \ldots, N\}$ is a positive integer corresponding to the best segmentation algorithm for an image x_k.

The SVM represents all training data D as points in multidimensional space. As a SVM is designed for two class classification,

assume jth ($j = 1, 2, \ldots, N$) algorithm as class one and the other $(N-1)$ algorithms as class two. The SVM determines the maximum-margin hyperplane svm_j to separate class one and class two. Maximum-margin hyperplane or classifier is given by (7).

$$svm_j = w_j \cdot x + b_j = 0 \tag{7}$$

where '·' denotes the dot product, w_j is a p-dimensional normal vector perpendicular to the hyperplane, and b_j is a offset of hyperplane from the origin along the w_j.

The normal vector w_j and offset parameter b_j are given by (8) and (9), respectively:

$$w_j = \sum_{i=1}^{k} \alpha_i C_i x_i, \tag{8}$$

$$b_j = \frac{1}{N_s} \sum_{i=1}^{N_s} (w_j \cdot x_i - C_i), \tag{9}$$

where $C_i = \left\{ \begin{array}{ll} -1 & \text{for } i = 1, 2, \ldots, j-1, j+1, \ldots, k \\ 1 & \text{for } i = j \end{array} \right\}$, α is the non-negative Lagrange multiplier and N_s is number of support vectors. Support vectors are the closest data points to maximum-margin hyperplane [36].

For N algorithms, N SVM classifiers svm_j ($j = 1, 2, \ldots, N$) are formed. Finally, the SVM model file is created with all N classifiers.

5.2. Validating the SVM

SVM validating procedure is illustrated in Fig. 4. In the beginning, validation data is created by using image histogram of the images. This data format is of the below form, assuming m validation images:

$$D_v = \{x_1^v, x_2^v, \ldots, x_m^v\}^T, \tag{10}$$

where x_m^v is the histogram of mth validating image represented in the form of p-dimensional real vector.

Validation images along with model files (created during training state) are used by SVM for predicting the suitable algorithm for these images. For kth (k is integer ranging from 1 to m) validation sample, SVM reads the model file and determines:

$$d_j(x) = w_j \cdot x_k^v + b_j, \quad \text{for } j = 1, 2, \ldots, N, \tag{11}$$

where w_j and b_j are the weight vector and offset value of svm_j classifier, which are obtained from model file.

Fig. 5. GUI for PM characterization.

For kth validation sample, Nth algorithm is the optimal algorithm if:

$$d_N(x) = \max_{j=1 \text{ to } N} d_j(x). \tag{12}$$

These steps are repeated for all validation images (*i.e.* for $k = 1$ to m) and finally a prediction file is generated, which consists of all predicted algorithms for the given image.

5.3. Designed software

A graphical user interface (GUI) is developed using image processing techniques and a SVM for analyzing particles images. A snapshot of the GUI is shown in Fig. 5. Like other image processing software, this GUI is provided with basic image processing tools such as reading, editing, preprocessing. In addition, it has the unique capability of selecting the best image segmentation method based on image features using SVM. GUI can be used to determine the particle features such as size, shape, area.

5.4. Results: examples of selecting optimal image segmentation algorithm using SVM

The efficiency of a SVM in predicting the optimal image segmentation algorithm from a set of algorithms is presented here. Five different algorithms (Otsu thresholding [37], Kapur thresholding [38], Rosin thresholding [39], Concavity thresholding [40], and extended Sobel edge detection method) are considered in this

Table 3
Results showing efficiency of SVM in predicting the optimal algorithm from a set of two, three and five algorithms.

No. of algorithms	No. of training images	No. of validating images	No. of images with correct prediction	No. of images with incorrect prediction	Efficiency (%)
2	10	25	18	7	72
	20	40	30	10	75
	25	25	20	5	80
	35	30	24	6	80
	45	25	21	4	84
3	10	25	16	9	64
	20	40	27	13	67
	25	25	18	7	72
	35	30	22	8	73
	45	25	20	5	80
5	10	25	15	10	60
	20	40	24	16	60
	25	25	16	9	64
	35	30	20	10	67
	45	25	17	8	68

Fig. 6. Comparison of SVM predicted algorithm with other methods: (a) SEM image of collected particles on filter paper, (b) SVM predicted method (Kapur thresholding) output, (c) Otsu thresholding output.

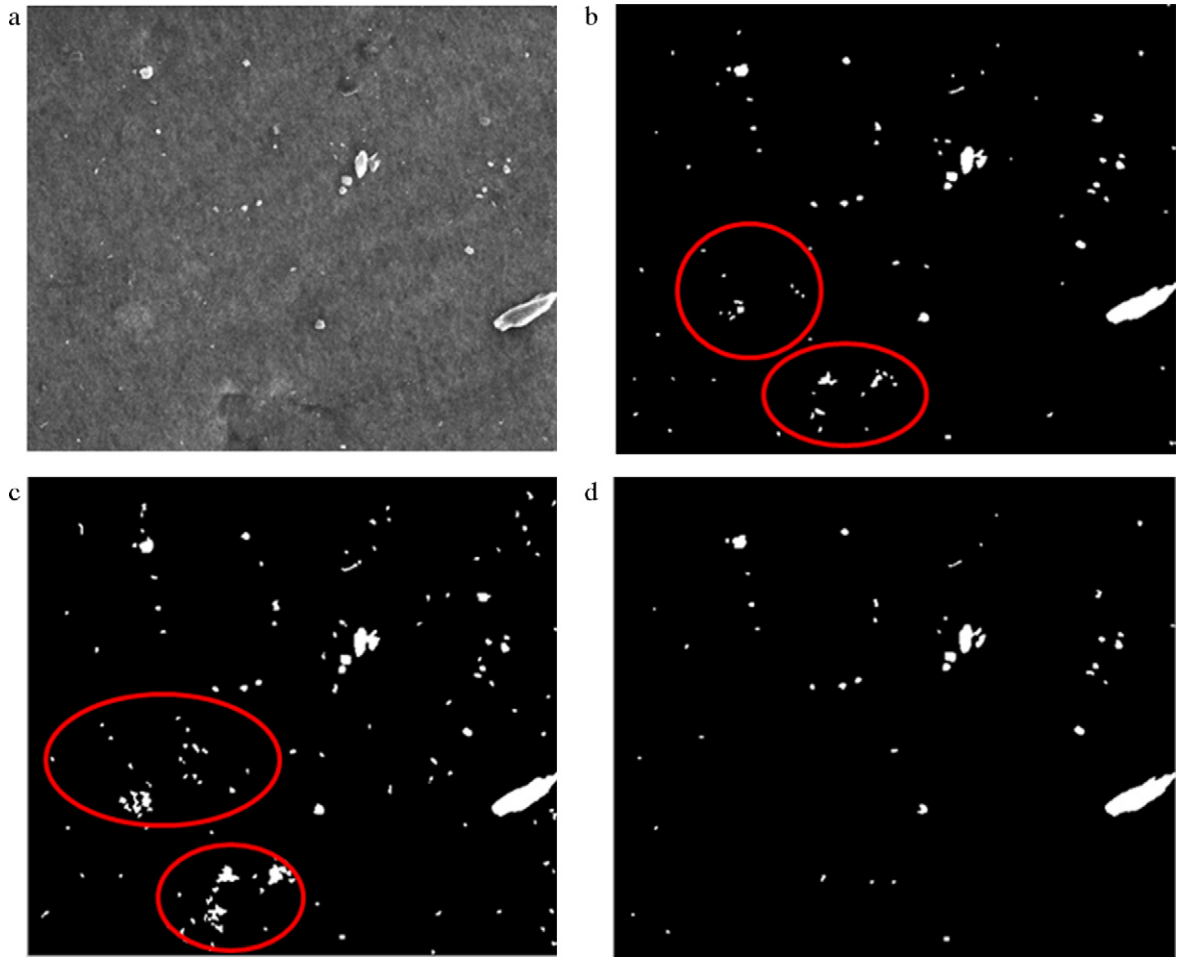

Fig. 7. Comparison of SVM predicted algorithm with other methods: (a) SEM image of particles, (b) Kapur thresholding output, (c) Rosin thresholding method output, (d) SVM predicted method (Otsu thresholding) output.

Table 4
Comparison of SVM predicted method with other methods in estimating the number of particles in image.

	Image used	Number of particles estimated by each segmentation method					
		Actual	Kapur thresholding	Otsu thresholding	Rosin thresholding	Concavity thresholding	Extended Sobel edge detection method
Case 1	Fig. 6(a)	40	33[a]	346	–	–	–
Case 2	Fig. 7(a)	41	83	44[a]	328	–	–
Case 3	Fig. 8(a)	62	20	81	328	273	56[a]

[a] SVM predicted method.

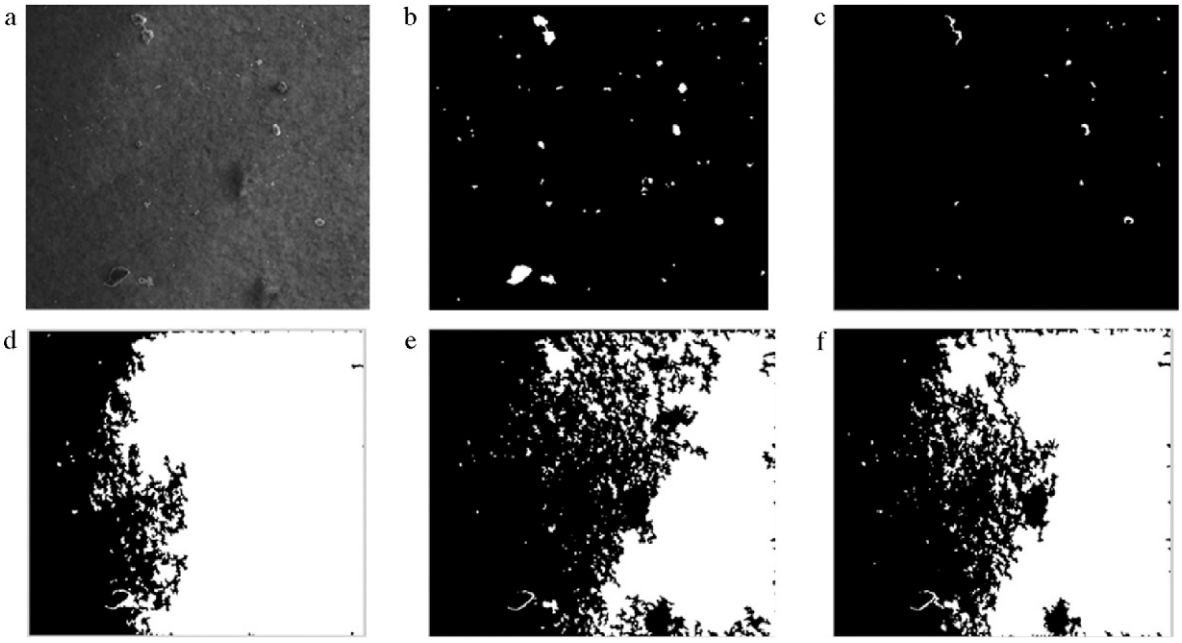

Fig. 8. Comparison of SVM predicted algorithm with other methods: (a) SEM image of particles, (b) output of SVM predicted method (extended Sobel edge detection method), (c) output of Kapur thresholding method, (d) output of Otsu thresholding method, (e) output of Rosin thresholding method, (f) output of concavity thresholding method.

study. In case 1, two different segmentation algorithms are used while for case 2, three different segmentation algorithms are used to study the efficiency of SVM. In case 3, five different segmentation algorithms are incorporated to study the efficiency of SVM. Table 3 shows the efficiency of SVM in predicting the optimal segmentation algorithm for each case. Figs. 6–8 show the comparison of SVM selected algorithm with other algorithm for case 1, case 2 and case 3 respectively. The red circled regions in Fig. 7 shows the inaccuracy of the algorithms in identifying the particles. From Table 4, it can be observed that SVM predicted algorithm is able to better estimate the number of particles than other methods.

6. Conclusion

In this paper, we proposed and illustrated a novel SEM integrated with image processing technique based on SVM for identifying and characterizing the particulate matter. The SVM method showed encouraging results in automating the selection of the best segmentation algorithm and thus automates the process of particle identification and characterization of particulate matter. Results show that SVM method provides an accuracy of 68% for selecting the best segmentation algorithm from a set of five algorithms, 80% for selecting the best segmentation algorithm from a set of three algorithms and 84% for selecting the best algorithm from a set of two algorithms. Further, it is observed that, even with a fewer number of training images, the SVM method showed satisfactory performance in predicting the best segmentation algorithm.

In the future, the SVM method can be applied to other image processing problems. For example, this method can be extended to select the best noise reduction method for an image based on its features. In this paper a gray level histogram is used as an image feature to train the SVM. Future researchers can investigate other image features to train the SVM.

Acknowledgments

The authors would like to thank Dr. F. Akbar and Dr. K. Czajkowski of the University of Toledo for incorporating particulate data collection into their field study. Financial support from the EECS Department and the U.S. Department of Agriculture is gratefully acknowledged. Filter images considered in the various examples were provided by Mr. A. Bhat, PhD candidate, working on characterization of particulate matter emitted during land application of biosolids. Dr. Devabhaktuni acknowledges the valuable reviews provided by Dr. M. Deo of the University of Michigan (Ann Arbor, USA). The views expressed in this paper are those of the authors.

References

[1] Particulate Matter, http://www.epa.gov/pm.
[2] D.J. Jasminka, Physical and chemical characterization of PM suspended in aerosols from the urban area of Belgrade, J. Serb. Chem. Soc. 74 (2009) 1319–1333.
[3] N. Englert, Fine particles and human health—a review of epidemiological studies, Toxicol. Lett. 149 (2004) 235–242.
[4] R.D. Peng, H.H. Chang, M.L. Bell, A. McDermott, S.L. Zeger, J.M. Samet, F. Dominici, Coarse PM air pollution and hospital admissions for cardiovascular and respiratory diseases among medicare patients, J. Am. Med. Assoc. 299 (2008) 2172–2179.
[5] M.J. Vallius, J. Ruuskanen, A. Mirme, J. Pekkanen, Concentrations and estimated soot content of PM_1, $PM_{2.5}$ and PM_{10} in sub-arctic urban atmosphere, Environ. Sci. Technol. 34 (2000) 1919–1925.
[6] P. Kothai, P. Prathibha, I.V. Saradhi, G.G. Pandit, V.D. Puranik, Characterization of atmospheric particulate matter using PIXE technique, Int. J. Environ. Sci. Technol. 1 (2009) 27–30.
[7] C. Davidson, P. Robert, S. Paul, Airborne particulate matter and human health: a review, Aerosol Sci. Technol. 39 (2005) 737–749.
[8] K. Shandilya, A. Kumar, Morphology of single inhalable particle inside public transit biodiesel fueled bus, J. Environ. Sci. 22 (2010) 263–270.
[9] E. Andrews, et al., Concentration and composition of atmospheric aerosols from the 1995 SEAVS experiment and a review of the closure between chemical and gravimetric measurements, J. Air Waste Manage. 50 (2000) 648–664.
[10] L.E. Ranweiler, J.L. Moyers, Atomic absorption procedure for analysis of metals in atmospheric particulate matter, Environ. Sci. Technol. 8 (1974) 152–156.
[11] M.N. Kayali, S. Rubio-Barroso, L.M. Polo-Diez, Rapid PAH determination in urban particulate air samples by HPLC with fluorometric detection and programmed excitation and emission wavelength pairs, J. Chromatogr. Sci. 33 (1995) 139–142.
[12] J.O. Allen, N.M. Dookeran, K.A. Smith, A.F. Sarofim, K. Taghizadeh, A.L. Lafleur, Measurement of PAHs associated with size-segregated atmospheric aerosols in Massachusetts, Environ. Sci. Technol. 30 (1996) 1023–1031.
[13] H.H. Yang, S.O. Lai, L.T. Hsieh, H.J. Hsueh, T.W. Chi, Profiles of PAH emission from steel and iron industries, Chemosphere 48 (2002) 1061–1074.
[14] J.F. Gomes, A simple way to measure particle size in flue gases, Chem. Eng. 105 (1998) 117–122.

[15] H.V. Malderen, R.V. Grieken, N.V. Bufetov, K.P. Koutzenogii, Chemical characterization of individual aerosol particles in central Siberia, Environ. Sci. Technol. 30 (1996) 312–321.
[16] T. Armstrong, R. Buseck, Quantitative chemical analysis of individual micro particles using the electron microprobe theoretical, Anal. Chem. 47 (1975) 2178–2192.
[17] G.S. Casuccio, S.F. Schlaegle, T.L. Lersch, G.P. Huffman, Y. Chen, N. Shah, Measurement of fine particulate matter using electron microscopy techniques, Fuel Process. Technol. 85 (2004) 763–779.
[18] Y. Mamane, R. Willisand, T. Conner, Evaluation of CCSEM applied to an ambient urban aerosol sample, Aerosol Sci. Technol. 34 (2001) 97–107.
[19] J.P. Zingerman, S.C. Mehta, J.M. Salter, G.W. Radebaugh, Validation of a computerized image analysis for particle size determination pharmaceutical applications, Int. J. Pharm. 88 (1998) 303–312.
[20] A.M. Nazar, F.A. Silva, J.J. Ammann, Image processing for particle characterization, Mater. Charact. 30 (1996) 165–173.
[21] Y.J. Zhang, A survey on evaluation methods for image segmentation, Pattern Recogn. 29 (1996) 1335–1346.
[22] K.S. Fu, J.K. Mui, A survey on image segmentation, Pattern Recogn. 13 (1981) 3–16.
[23] J.M. Korath, A. Abbas, J.A. Romagnoli, A clustering approach for the separation of touching edges in particle images, Part. Part. Syst. Charact. 25 (2008) 143–152.
[24] R. Strandh, J.O. Lapeyre, An efficient union-find algorithm for extracting the connected components of a large-sized image, http://citeseerx.ist.psu.edu/viewdoc.
[25] A. Bieniek, A. Moga, An efficient watershed algorithm based on connected components, Pattern Recogn. 33 (2000) 907–916.
[26] R.C. Gonzalez, R.E. Woods, Digital Image Processing, Addision-Weseley Publication Company, USA, 2008.
[27] F. Podczeck, A shape factor to assess the shape of particles using image analysis, Powder Technol. 93 (1997) 47–53.
[28] ImageJ, US National Institutes of Health, USA, http://rsb.info.nih.gov/nih-imageJ.
[29] Scanning Probe Image Processor, Image Metrology, Denmark, http://www.imagemet.com.
[30] Pax-it image analysis software, USA, http://www.paxit.com/paxit/particle_size_analysis.
[31] Clemex Vision PE, Clemex intelligent microscopy, Quebec, Canada, http://www.clemex.com/Products/ImageAnalysis/Software/VisionPE.aspx.
[32] P.I. Smart, Carl Zeiss, http://www.smt.zeiss.com/maximum-particleanalysis.
[33] Image Pro, MediaCybernetics, USA, http://www.mediacy.com/index.aspx?page=IPP.
[34] L. Spirkovska, A Summary of Image Segmentation Techniques, Ames. Research Center, Moffett Field, NASA Technical Memorandum 104022, USA, 1993.
[35] X. Yong, D. Feng, Z. Rongchum, M. Petrou, Learning-based algorithm selection for image segmentation, Pattern Recogn. Lett. 6 (2005) 1059–1068.
[36] C. Cortes, V. Vapnik, Support vector networks, Mach. Learn. 20 (1995) 273–297.
[37] N. Otsu, A threshold selection method from gray-level histogram, IEEE Trans. Syst. Man. Cyb. 9 (1979) 62–66.
[38] J.N. Kapur, P.K. Sahoo, A.K.C. Wong, A new method for gray-level picture thresholding using the entropy of the histogram, Comput. Vision Graph. 29 (1985) 273–285.
[39] P.L. Rosin, Unimodal thresholding, Pattern Recogn. 34 (2001) 2083–2096.
[40] A. Rosenfeld, P. Torre, Histogram concavity analysis as an aid in threshold selection, IEEE Trans. Syst. Man. Cyb. 13 (1983) 231–235.